


NANO EXPRESS

Open Access



Prediction of Quantum Anomalous Hall Effect in MBi and MSb (M:Ti, Zr, and Hf) Honeycombs

Zhi-Quan Huang^{1†}, Wei-Chih Chen^{1†}, Genevieve M. Macam^{1†}, Christian P. Crisostomo¹, Shin-Ming Huang¹, Rong-Bin Chen³, Marvin A. Albao⁴, Der-Jun Jang^{1,2}, Hsin Lin^{5,6,7} and Feng-Chuan Chuang^{1,2*} 

Abstract

The abounding possibilities of discovering novel materials has driven enhanced research effort in the field of materials physics. Only recently, the quantum anomalous hall effect (QAHE) was realized in magnetic topological insulators (TIs) albeit existing at extremely low temperatures. Here, we predict that MPn (M=Ti, Zr, and Hf; Pn=Sb and Bi) honeycombs are capable of possessing QAH insulating phases based on first-principles electronic structure calculations. We found that HfBi, HfSb, TiBi, and TiSb honeycomb systems possess QAHE with the largest band gap of 15 meV under the effect of tensile strain. In low-buckled HfBi honeycomb, we demonstrated the change of Chern number with increasing lattice constant. The band crossings occurred at low symmetry points. We also found that by varying the buckling distance we can induce a phase transition such that the band crossing between two Hf d-orbitals occurs along high-symmetry point K2. Moreover, edge states are demonstrated in buckled HfBi zigzag nanoribbons. This study contributes additional novel materials to the current pool of predicted QAH insulators which have promising applications in spintronics.

Keywords: Quantum anomalous Hall effect, Topological phase transition, TM-Bi honeycomb, Electronic structures, First-principles calculations

Background

Rigorous research efforts have been continuously focused towards the exploration of novel 2D materials such as quantum spin Hall (QSH) insulators. These novel materials, also known as two-dimensional topological insulators (2D TIs) exhibit a unique property wherein the edges possess spin-polarized gapless states despite the bulk system being an insulator [1]. QSH insulators show dissipationless spin/charge transport which is highly important in spintronic device applications [2]. Recently, it has been discovered that the breaking of time-reversal symmetry (TRS) in QSH insulators lead to a quantum anomalous

Hall effect (QAHE) system in which helical edge states are converted into chiral edge states [3]. The dissipationless charge transport without the need for an external magnetic field provides promising applications in low energy consumption spintronics [4, 5] and has encouraged the search for more QAHE systems [6, 7]. Predicted by Haldane in 1988, QAHE was only experimentally achieved in 2013 by magnetically doping thin films of topological insulators [8]. Theoretical studies have suggested that the quantum anomalous Hall (QAH) phase can be achieved by breaking the TRS of a TI by introducing ferromagnetism and inducing a band inversion transition by strong spin-orbit coupling (SOC) effects [9, 10]. Thus, QSH insulators are good starting materials to achieve QAHE. Several studies have predicted that thin films of groups IV (Sn) [11–13] and V (Bi, Sb) [6, 14–17] support QSH phases which can also be achieved via chemical functionalization [17, 18]. Besides group IV and V elements, it was also predicted that [19–21] III-V honeycombs support

*Correspondence: fchuang@mail.nsysu.edu.tw

†Equal contributors

¹Department of Physics, National Sun Yat-Sen University, Kaohsiung 804, Taiwan

²Multidisciplinary and Data Science Research Center, National Sun Yat-Sen University, Kaohsiung 804, Taiwan

Full list of author information is available at the end of the article

the QSH phase in both freestanding and functionalized cases. These results paved the way for finding QAHE phases. Studies have shown that QAHE were found to exist in functionalized group IV [22] and V [17, 18, 22] thin films. In addition, first-principles calculations show QAHE in fluorinated [23] and chemically functionalized [24] III-V honeycombs. Moreover, several theoretical studies have predicted that transition metals doping in honeycombs can induce QAH phases [17, 25–27]. This has been experimentally realized via Cr and V doping [8, 28, 29]. Supported by the finding that III-V honeycomb materials are QSH insulators [19] and the theoretical prediction that doping a magnetic material can induce magnetism [10], we replace the group III element with a transition metal (M=Ti, Zr, and Hf). Transition-metal carbides MC (M=Zr and Hf) [30] and transition-metal halides MX (M=Zr and Hf) [31] are also another family of materials predicted to exist as QSH insulators. However, its potential to support QAHE has not been explored yet. Motivated by these findings, we predict the electronic properties of transition-metal pnictides MPn (M=Ti, Zr, and Hf; Pn=Sb and Bi) to exhibit the QAH phase. In this work, we employ first-principles calculations to predict the ability of transition metals (M=Ti, Zr, and Hf) to induce intrinsic magnetism on Bi/Sb honeycombs. We examine both buckled and planar cases and identify the phase changes due to strain. The QAH phases are verified by calculating the Chern number and observing band inversion.

Results and Discussions

Similar to pure Bi honeycomb (with two atoms in the unit cell) which can adopt both buckled and planar structures, our material is obtained by replacing half of Bi by a transition metal [e.g., Ti, Zr, and Hf] in the unit cell. The top

view of M-Bi/Sb with an outlined 1×1 unit cell is shown in Fig. 1a, while the side views of buckled and planar M-Bi/Sb honeycombs are shown in Fig. 1b, c, respectively. The corresponding first Brillouin zone (BZ) labeled with high-symmetry points is shown in Fig. 1d.

We study the stability of honeycombs and the effect of strain by varying the lattice constant and allowing the atoms to relax for both buckled and planar cases. Next, we identified their topological phases under different strains through the Chern number calculations. The result is illustrated via a phase diagram as presented in Fig. 2. The energy curves for TiBi, ZrBi, and HfBi are shown in Fig. 2a–c, respectively. We found that MBi honeycombs possess the low-buckled and planar phases. Through these figures, we identify the equilibrium lattice constants for further analysis. The figure also shows that buckled MBi is the energetically favored structure. However, most of the QAH phases are observed when the strain is increased which transforms the material from buckled to planar honeycombs. It should also be noted that QAH phases could be observed in buckled HfBi but only within a small range of lattice constants [see Fig. 2c].

Tables 1 and 2 show the equilibrium lattice constants for M-Bi and M-Sb structures. The associated band gap, magnetic moment, phase, and material classification are also indicated. QAHE is present when the calculated Chern number, C , is a non-zero integer. The band gap is calculated as the difference between the lowest unoccupied and the highest occupied bands. Our calculations show that the QAH insulator phase can be found in planar TiBi and HfBi with band gaps of 15 and 7 meV, respectively. Moreover, phase transition can be induced in TiBi by varying the buckled distance [see Fig. 3] and by inducing strain in buckled HfBi [Fig. 4]. In TiBi, we find that the band

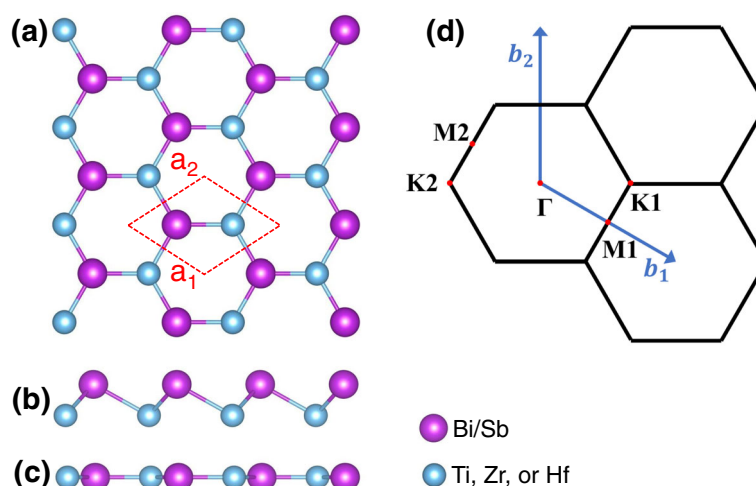
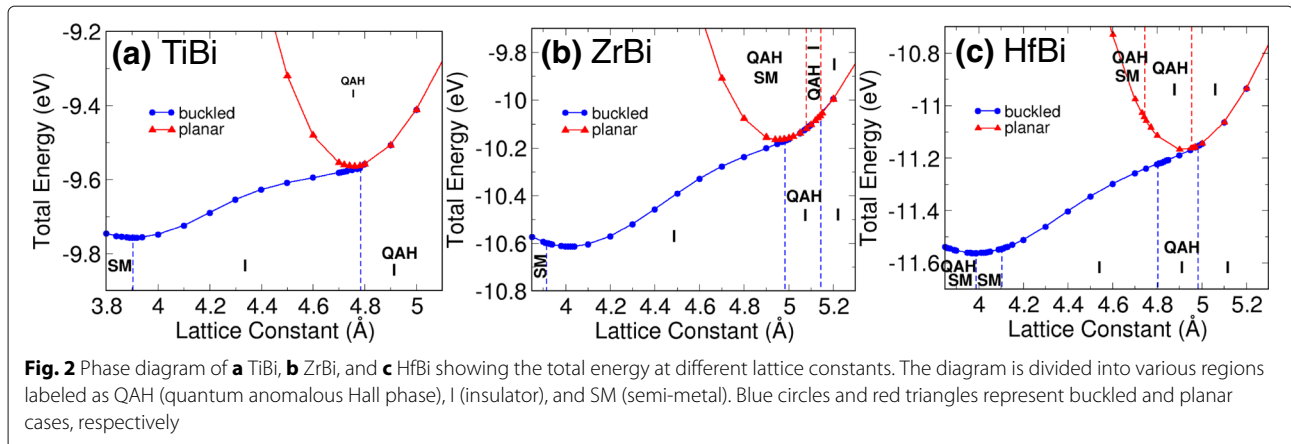


Fig. 1 **a** Crystal structure of M-Sb/Bi honeycomb. **b, c** Side views of buckled and planar structures, respectively. **d** The first Brillouin zone (BZ) with high-symmetry points



crossings due to the varying of buckling distance occur at low symmetry points shown in Fig. 3d; while in HfBi, we observed the two band crossings (critical transition points) first at K2 ($a = 4.8 \text{ \AA}$) and then at K1 ($a = 5.0 \text{ \AA}$) due to strain in Fig. 4c, g.

Figure 5a, b shows the electronic band structures at equilibrium lattice constants for M-Bi and M-Sb in planar and buckled structures, respectively. The red and blue circles are the spin up and spin down contributions, respectively. The QAH phase (with $C = 1$) with largest band gap is 15 meV observed in planar TiBi. Planar HfBi is also a QAH insulator with a small band gap of 7 meV (with $C = -1$). However, in a buckled form, HfBi is a semi-metal with a high $C = -3$. On the other hand, buckled ZrBi, TiSb, ZrSb, and planar ZrSb are found to be trivial insulators.

The nature of QAHE can be further understood by examining the effects of SOC in non-magnetic and ferromagnetic calculations. For this purpose, we chose planar TiBi (with $a = 4.76 \text{ \AA}$) as the exemplar. The band structures obtained in non-magnetic and ferromagnetic calculations with and without SOC are shown in Fig. 6. Our calculations show that this structure has a

magnetic moment of $1.05 \mu_B$ per unit cell which is mainly contributed by Ti atoms. In the non-magnetic calculations, we find that the system is metallic [Fig. 6a, c]. We can observe in Fig. 6b that a net magnetic moment can be induced due to ferromagnetic ordering which is influenced by the transition metal, Ti. Furthermore, the system now has gapless spin-up states (red lines) and gapped spin-down states, and by applying SOC to the ferromagnetic calculation, a gap of 15 meV is then obtained. This shows that the band inversion is induced by SOC and the gap opening results in QAHE.

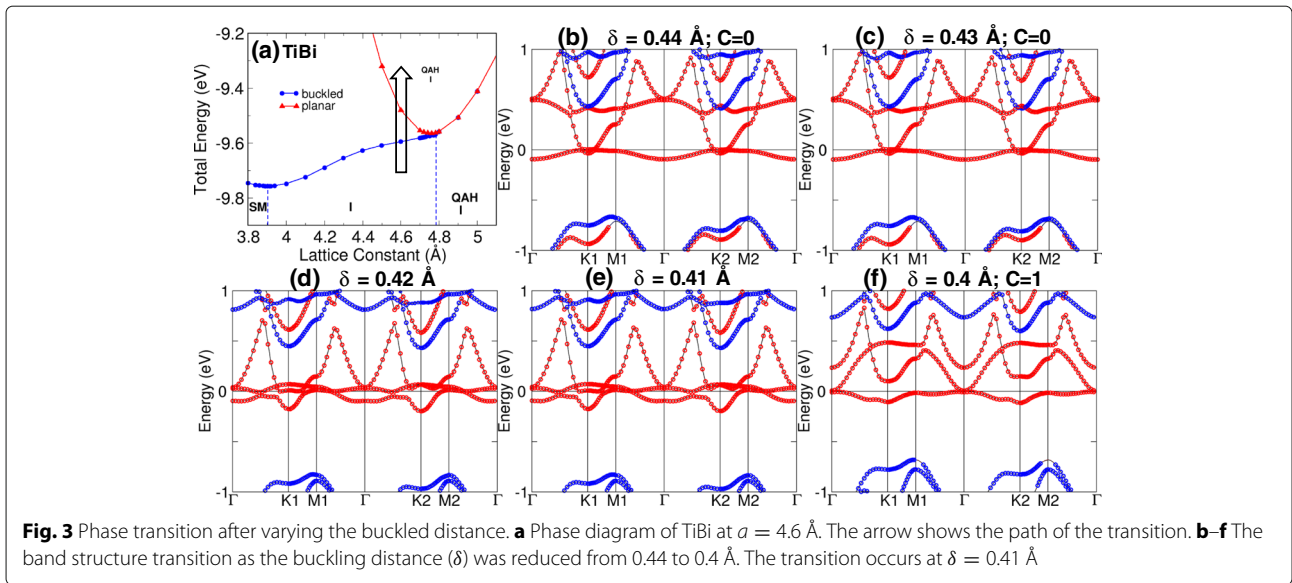
Finally, we inspect the edge band spectrum of planar HfBi honeycomb for the presence of edge states using tight-binding Hamiltonians derived via Wannier functions. We constructed HfBi ribbons with zigzag edges and width of 127 \AA as shown in Fig. 7. The figure also confirms the presence of edge states denoted by and proportional to the size of the red and blue circles which represent the right and left edges, respectively. The separate edge states are due to the asymmetry of the right and left zigzag edges. We can also observe an odd number of edge band crossing the fermi level. We find that this number is the same as the absolute value of the

Table 1 Calculated equilibrium lattice constants, system band gaps, magnetic moment, and topological phase of planar and buckled M-Bi honeycombs

	M-Bi	Lattice constant (Å)	Band gap (meV)	Phase	Classification	Mag. (μ_B)
Planar	TiBi	4.76	15	QAH	Insulator	1.050
	ZrBi	4.96	-3	QAH	Semi-metal	1.005
	HfBi	4.92	7	QAH	Insulator	0.947
Buckled	TiBi	3.9	-12	-	Semi-metal	1.085
	ZrBi	4.01	10	-	Insulator	1.046
	HfBi	3.98	-54	QAH	Semi-metal	1.005

Table 2 Calculated equilibrium lattice constants, system band gaps, magnetic moment, and topological phase of planar and buckled M-Sb honeycombs

	M-Sb	Lattice constant (Å)	Band gap (meV)	Phase	Classification	Mag. (μ_B)
Planar	TiSb	4.64	-70	QAH	Semi-metal	1.004
	ZrSb	4.84	8	-	Insulator	0.996
	HfSb	4.82	-50	-	Metal	0.948
Buckled	TiSb	3.81	256	-	Insulator	1.007
	ZrSb	3.94	230	-	Insulator	1.003
	HfSb	3.92	-59	QAH	Semi-metal	0.979



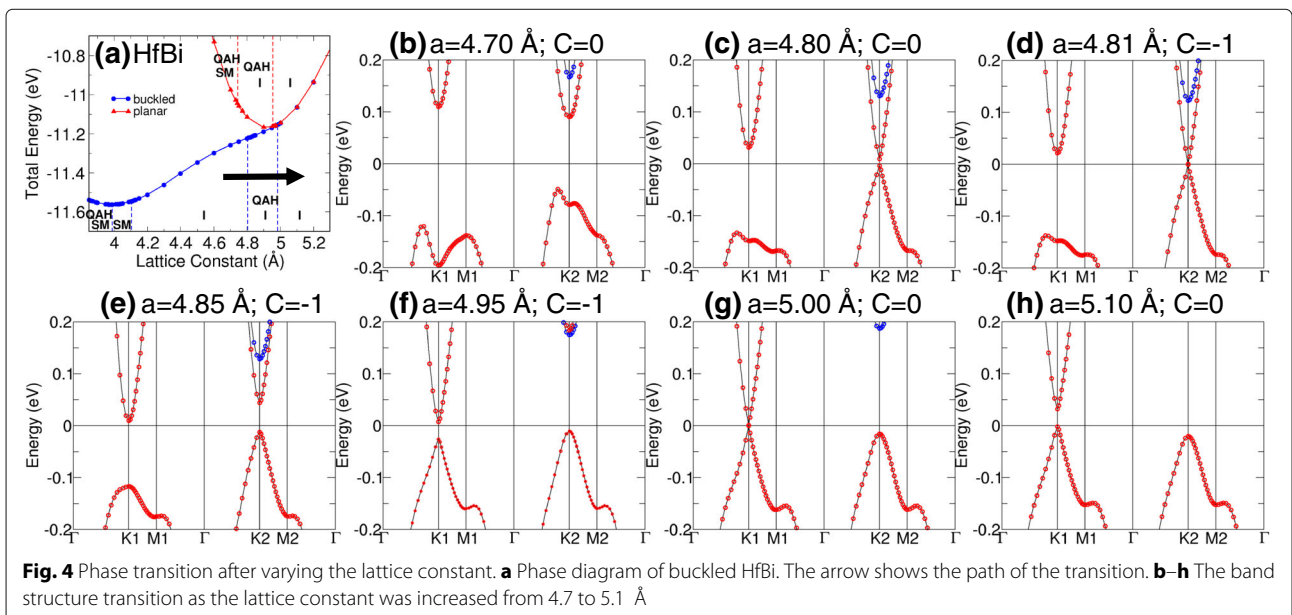
Chern number, further confirming the QAH phase in planar HfBi.

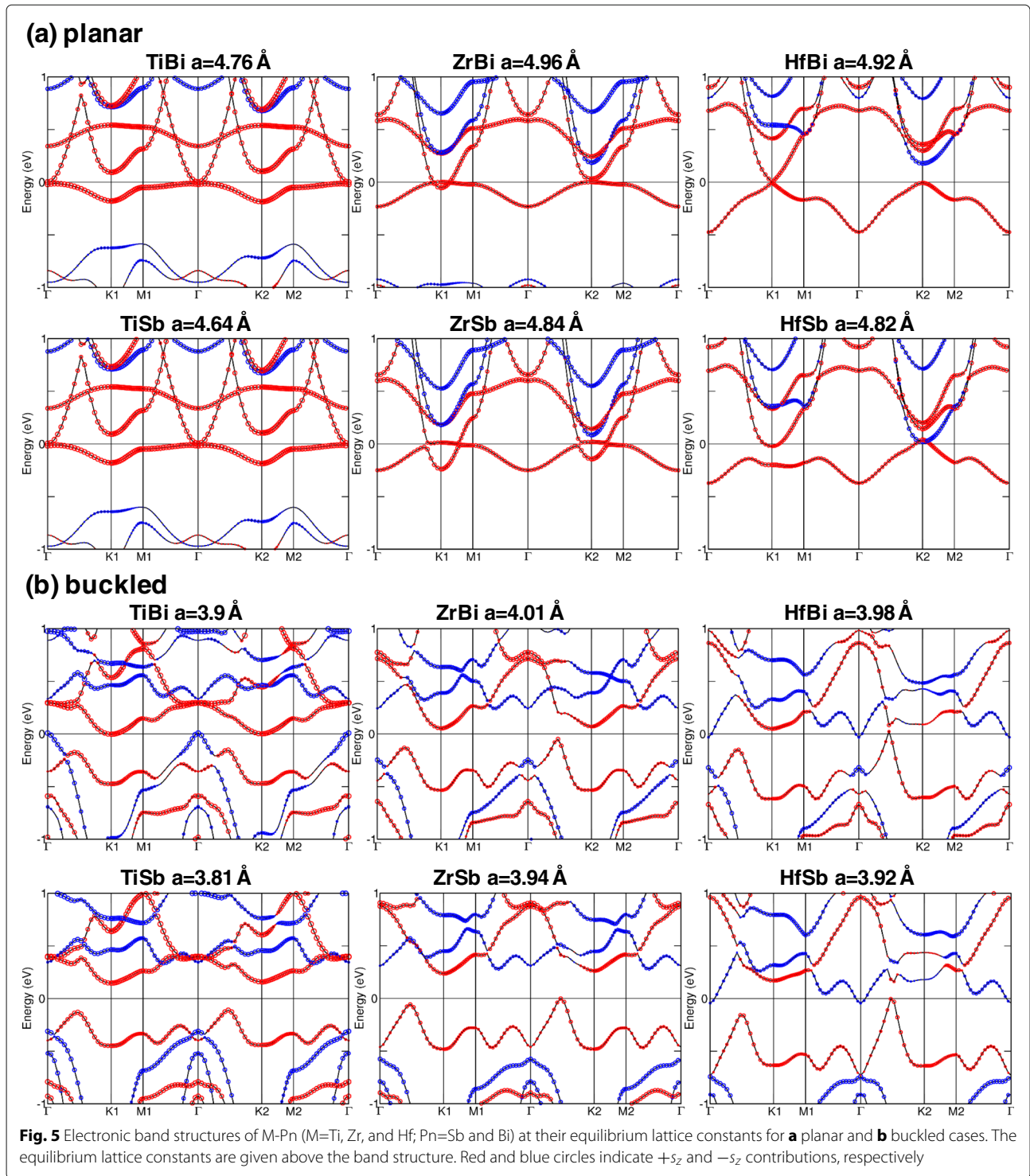
We have further calculated the phonon spectrum for each system and noted that these systems possessed negative frequency. Thus, the aforementioned systems would need a substrate to stabilize. We also noted that the aforementioned calculations were done using a one by one unit cell, and the materials with ferromagnetic (FM) configuration is the most stable state. However, for a larger supercell, we found that FM still has a lower energy than the anti-ferromagnetic (AFM)

configuration in the buckled cases, while both FM and AFM configurations are degenerate in energy in the planar cases.

Conclusions

To summarize, our first-principles calculations predict that the replacement of transition metals (Ti, Zr, and Hf) on Sb or Bi honeycomb films could potentially exhibit the QAH phase. Although these materials are energetically more stable in their buckled form, transforming it to planar form yields the QAH phase in a quite reasonable





range of lattice constants. Such phase can also be induced by varying the buckling distance and by applying strain as should in our calculated phase diagrams. We find that planar TiBi and HfBi structures exist as QAH insulators with a band gap of 15 and 7 meV, respectively. These findings offer another way of realizing the QAH phase in

honeycomb materials which could potentially be of use in spintronic applications.

Methods/Experimental

First-principles calculations within the density functional theory (DFT) framework were performed using the

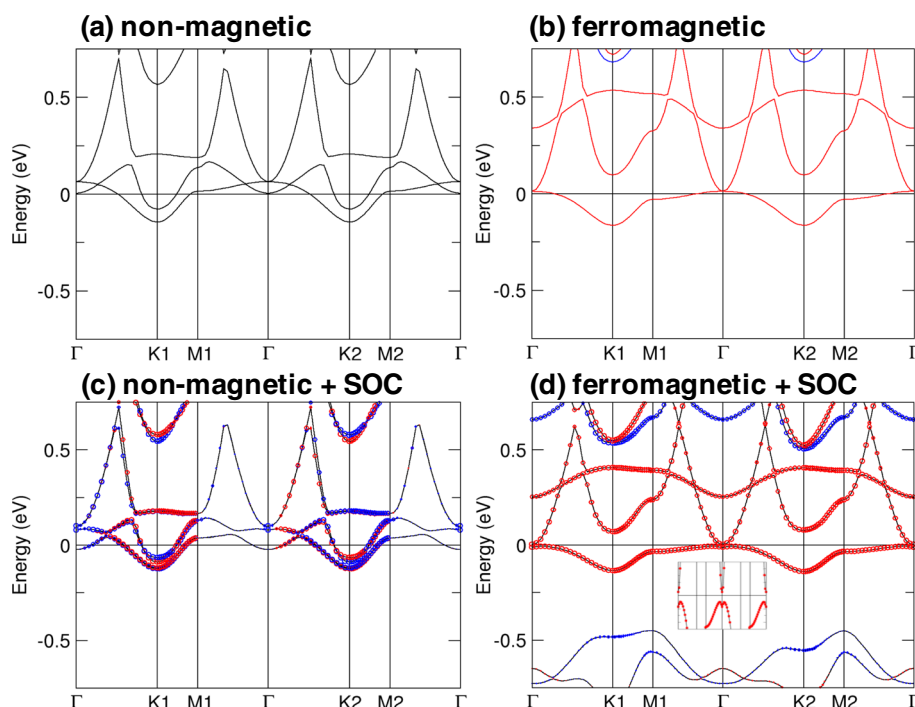


Fig. 6 Electronic band structures of planar TiBi film at $a = 4.76 \text{ \AA}$ for non-magnetic calculations (a) without SOC and (c) with SOC as well as ferromagnetic calculations (b) without SOC and (d) with SOC. Red and blue circles indicate $+s_z$ and $-s_z$ contributions, respectively, for (c) non-magnetic (d) ferromagnetic) calculations with SOC

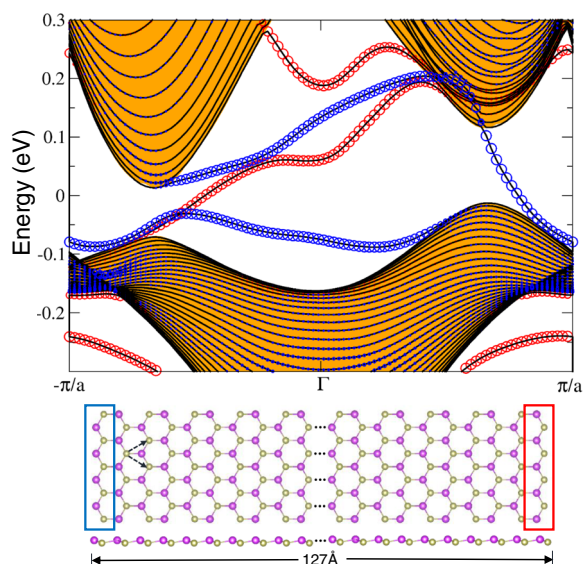


Fig. 7 Band structure along the edge of buckled HfBi zigzag nanoribbon with $a = 4.9 \text{ \AA}$ and the width of 127 \AA . Blue (red) circles indicate the contribution from the left (right) edges. The bulk bands are denoted by the orange-filled region

generalized gradient approximation (GGA) [32–36] and projector-augmented-wave (PAW) [37] method as implemented in the Vienna Ab-Initio Simulation Package Version 5.3 (VASP) [38, 39]. The kinetic energy cutoff was set to 350 eV and the crystal structures were optimized until the residual forces were no greater than $5 \times 10^{-3} \text{ eV/\AA}$. The self-consistency criteria for convergence was set at 10^{-6} eV for electronic structure calculations with or without spin-orbit coupling. We simulate a thin film by inserting a vacuum layer of at least 20 \AA along the z direction on a sampled 2D Brillouin zone of $24 \times 24 \times 1$ Gamma-centered Monkhorst-Pack grids [40]. We calculated the maximally localized Wannier functions using the WANNIER90 package [41] which were then used to calculate edge states. The topological phases were identified by calculating the Chern number using Z2Pack package [42, 43] which utilizes a technique that will track hybrid Wannier charge centers.

Acknowledgements

FCC acknowledges support from the National Center for Theoretical Sciences and the Ministry of Science and Technology of Taiwan under Grants No. MOST-104-2112-M-110-002-MY3 and the support under NSYSU-NKMU Joint Research Project Nos. 105-P005 and 106-P005. He is also grateful to the National Center for High-performance Computing for computer time and facilities. SMH is supported by the Ministry of Science and Technology in Taiwan under Grant

No. MOST-105-2112-M-110-014-MY3. HL is supported by the National Research Foundation Singapore under Grant No. NRF-NRFF2013-03.

Authors' contributions

FCC and HL conceived and initiated the study. WCC, CPC, ZQH, and GMM performed first-principles calculations. ZQH performed the Chern number calculation and edge state calculations. CPC, GMM, WCC, ZQH, FCC, SMH, DJJ, RBC, MAA, and HL performed the detailed analysis and contributed to discussions. GMM, CPC, ZQH, FCC, and HL, wrote the manuscript. All authors reviewed the manuscript. All authors read and approved the final manuscript.

Competing interests

The authors declare that they have no competing interests.

Publisher's Note

Springer Nature remains neutral with regard to jurisdictional claims in published maps and institutional affiliations.

Author details

¹Department of Physics, National Sun Yat-Sen University, Kaohsiung 804, Taiwan. ²Multidisciplinary and Data Science Research Center, National Sun Yat-Sen University, Kaohsiung 804, Taiwan. ³Center of General Studies, National Kaohsiung Marine University, Kaohsiung 811, Taiwan. ⁴Institute of Mathematical Sciences and Physics, University of The Philippines Los Baños College, 811, Laguna, Philippines. ⁵Institute of Physics, Academia Sinica, Taipei 11529, Taiwan. ⁶Centre for Advanced 2D Materials and Graphene Research Centre, National University of Singapore, 6 Science Drive 2, Singapore 117546, Singapore. ⁷Department of Physics, National University of Singapore, 2 Science Drive 3, Singapore 117542, Singapore.

Received: 2 November 2017 Accepted: 25 December 2017

Published online: 07 February 2018

References

- Kane CL, Mele EJ (2005) Z₂ topological order and the quantum spin hall effect. *Phys Rev E* 95:146802
- Roth A, Brüne C, Buhmann H, Molenkamp LW, Maciejko J, Qi XL, Zhang SC (2009) Nonlocal Transport in the Quantum Spin Hall State. *Science* 325:294–297
- He K, Wang Y, Xue QK (2014) Quantum anomalous Hall effect. *Natl Sci Rev* 1(1):38–48
- Weng H, Yu R, Hu X, Dai X, Fang Z (2015) Quantum anomalous Hall effect and related topological electronic states. *Adv Phys* 64(3):227–282
- He K (2015) The Quantum Hall Effect Gets More Practical. *Physics* 8:41
- Hsu CH, Huang ZQ, Crisostomo CP, Yao LZ, Chuang FC, Liu YT, et al (2016) Two-dimensional Topological Crystalline Insulator Phase in Sb/Bi Planar Honeycomb with Tunable Dirac Gap. *Sci Rep* 6:18993
- Guterding D, Jeschke HO, Valentí R (2016) Prospect of quantum anomalous Hall and quantum spin Hall effect in doped kagome lattice Mott insulators. *Sci Rep* 6:25988
- Chang CZ, Zhang J, Feng X, Shen J, Zhang Z, Guo M, et al (2013) Experimental observation of the quantum anomalous hall effect in a magnetic topological insulator. *Science* 340(6129):167–170
- Qi XL, Hughes TL, Zhang SC (2008) Topological field theory of time-reversal invariant insulators. *Phys Rev B* 78(19):195424
- Yu R, Zhang W, Zhang HJ, Zhang SC, Dai X, Fang Z (2010) Quantized anomalous hall effect in magnetic topological insulators. *Science* 329(5987):61–64
- Xu Y, Yan B, Zhang HJ, Wang J, Xu G, Tang P, et al (2013) Large-gap quantum spin hall insulators in tin films. *Phys Rev Lett* 111(13):136804
- Chou BH, Huang ZQ, Hsu CH, Chuang FC, Liu YT, Lin H, et al (2014) Hydrogenated ultra-thin tin films predicted as two-dimensional topological insulators. *New J Phys* 16(11):115008
- Wang TC, Hsu CH, Huang ZQ, Chuang FC, Su WS, Guo GY (2016) Tunable magnetic states on the zigzag edges of hydrogenated and halogenated group-IV nanoribbons. *Sci Rep* 6:39083
- Liu CC, Guan S, Song Z, Yang SA, Yang J, Yao Y (2014) Low-energy effective Hamiltonian for giant-gap quantum spin Hall insulators in honeycomb X-hydride/halide (X=N-Bi) monolayers. *Phys Rev B* 90(8):085431
- Chen L, Cui G, Zhang P, Wang X, Liu H, Wang D (2014) Edge state modulation of bilayer Bi nanoribbons by atom adsorption. *Phys Chem Chem Phys (PCCP)* 16(32):17206–12
- Song Z, Liu CC, Yang J, Han J, Ye M, Fu B, et al (2014) Quantum spin Hall insulators and quantum valley Hall insulators of BiX/SbX (X=H, F, Cl and Br) monolayers with a record bulk band gap. *NPG Asia Materials* 6:e147
- Jin KH, Jhi SH (2015) Quantum anomalous Hall and quantum spin-Hall phases in flattened Bi and Sb bilayers. *Sci Rep* 5:8426
- Liu CC, Zhou JJ, Yao Y (2015) Valley-polarized quantum anomalous Hall phases and tunable topological phase transitions in half-hydrogenated Bi honeycomb monolayers. *Phys Rev B* 91(16):165430
- Chuang FC, Yao LZ, Huang ZQ, Liu YT, Hsu CH, Das T, et al (2014) Prediction of large-gap two-dimensional topological insulators consisting of bilayers of group III elements with Bi. *Nano Lett* 14(5):2505–2508
- Ma Y, Li X, Kou L, Yan B, Niu C, Dai Y, et al (2015) Two-dimensional inversion-asymmetric topological insulators in functionalized III-Bi bilayers. *Phys Rev B* 91(23):235306
- Li L, Zhang X, Chen X, Zhao M (2015) Giant topological nontrivial band gaps in chloridized gallium bismuthide. *Nano Lett* 15(2):1296–1301
- Hsu CH, Fang Y, Wu S, Huang ZQ, Crisostomo CP, Gu YM, et al (2017) Quantum anomalous Hall insulator phase in asymmetrically functionalized germanene. *Phys Rev B* 96(16):165426
- Chen SP, Huang ZQ, Crisostomo CP, Hsu CH, Chuang FC, Lin H, et al (2016) Prediction of Quantum Anomalous Hall Insulator in half-fluorinated GaBi Honeycomb. *Sci Rep* 6:31317
- Crisostomo CP, Huang ZQ, Hsu CH, Chuang FC, Lin H, Bansil A (2017) Chemically induced large-gap quantum anomalous Hall insulator states in III-Bi honeycombs. *npj Comput Mater* 3(1):39
- Qiao Z, Yang SA, Feng W, Tse WK, Ding J, Yao Y, et al (2010) Quantum anomalous Hall effect in graphene from Rashba and exchange effects. *Phys Rev B* 82(16):161414
- Kaloni TP, Singh N, Schwingenschlögl U (2014) Prediction of a quantum anomalous Hall state in Co-decorated silicene. *Phys Rev B* 89(3):035409
- Kaloni TP (2014) Tuning the structural, electronic, and magnetic properties of germanene by the adsorption of 3d transition metal atoms. *J Phys Chem C* 118(43):25200–25208
- Kou X, Guo ST, Fan Y, Pan L, Lang M, Jiang Y, et al (2014) Scale-invariant quantum anomalous hall effect in magnetic topological insulators beyond the two-dimensional limit. *Phys Rev Lett* 113(13):137201
- Chang CZ, Zhao W, Kim DY, Zhang H, Assaf BA, et al (2015) High-precision realization of robust quantum anomalous Hall state in a hard ferromagnetic topological insulator. *Nat Mater* 14:473–477
- Zhou L, Shao B, Shi W, Sun Y, Felser C, Yan B, et al (2016) Prediction of the quantum spin Hall effect in monolayers of transition-metal carbides MC (M = Ti, Zr, Hf). *2D Materials* 3(3):035022
- Zhou L, Kou L, Sun Y, Felser C, Hu F, Shan G, et al (2015) New family of quantum spin hall insulators in two-dimensional transition-metal halide with large nontrivial band gaps. *Nano Lett* 15(12):7867–7872
- Hohenberg P, Kohn W (1964) Inhomogeneous electron gas. *Phys Rev* 136(3B):B864–B871
- Kohn W, Sham LJ (1965) Self-Consistent Equations Including Exchange and Correlation Effects. *Phys Rev* 140(4A):A1133–A1138
- Ceperly DM, Alder BJ (1980) Ground State of the Electron Gas by a Stochastic Method. *Phys Rev Lett* 45(7):566–569
- Perdew JP, Zunger A (1981) Self-interaction correction to density-functional approximations for many-electron systems. *Phys Rev B* 23(10):5048–5079
- Perdew JP, Burke K, Ernzerhof M (1996) Generalized Gradient Approximation Made Simple. *Phys Rev Lett* 77(18):3865–3868
- Kresse G, Joubert D (1999) From ultrasoft pseudopotentials to the projector augmented-wave method. *Phys Rev B* 59(3):1758–1775
- Kresse G, Hafner J (1993) Ab initio molecular dynamics for liquid metals. *Phys Rev B* 47(1):558–561
- Kresse G, Furthmüller J (1996) Efficient iterative schemes for ab initio total-energy calculations using a plane-wave basis set. *Phys Rev B* 54(16):11169–11186
- Monkhorst HJ, Pack JD (1976) Special points for Brillouin-zone integrations. *Phys Rev B* 13(12):5188–5192
- Mostofi AA, Yates JR, Lee Y-s, Souza I, Vanderbilt D, Marzari N (2008) wannier90: A tool for obtaining maximally-localised Wannier functions. *Comput Phys Commun* 178(9):685–699

42. Soluyanov AA, Vanderbilt D (2011) Computing topological invariants without inversion symmetry. *Phys Rev B* 83(23):235401
43. Gresch D, Autès G, Yazyev OV, Troyer M, Vanderbilt D, Bernevig BA, et al (2017) Z2Pack: Numerical implementation of hybrid Wannier centers for identifying topological materials. *Phys Rev B* 95(7):075146

Submit your manuscript to a SpringerOpen[®] journal and benefit from:

- ▶ Convenient online submission
- ▶ Rigorous peer review
- ▶ Open access: articles freely available online
- ▶ High visibility within the field
- ▶ Retaining the copyright to your article

Submit your next manuscript at ▶ [springeropen.com](https://www.springeropen.com)
